Structural aspects of barium borosilicate glasses containing thorium and uranium oxides

R.K. Mishra [a], V. Sudarsan [b], C.P. Kaushik [a], Kanwar Raj [a],
S.K. Kulshreshtha [b], A.K. Tyagi [b],*

[a] *Waste Management Division, Bhabha Atomic Research Centre, Mumbai 400085, India*
[b] *Chemistry Division, Bhabha Atomic Research Centre, Mumbai 400085, India*

Abstract

Barium borosilicate glasses incorporated with 15.86 wt% ThO_2 and containing different amounts of uranium oxide were prepared by conventional melt quench method. Based on ^{29}Si and ^{11}B magic angle spinning nuclear magnetic resonance (MAS NMR) studies, it has been confirmed that uranium oxide incorporation is associated with distortion of borosilicate network as revealed by the increase in the relative concentration of Q^2 structural units of silicon as well as the increase in the quadrupolar coupling constant (C_q) of BO_3 structural units. The increased number of non-bridging oxygen atoms brought about by the increase in Q^2 structural units of silicon facilitates the incorporation of both uranium and thorium ions in the sites created by non-bridging oxygen atoms (network modifying positions) in the glass. Uranium oxide incorporation above 7.5 wt% resulted in the phase separation of ThO_2 as revealed by the X-ray diffraction studies. The present study focuses on the structural changes with the borosilicate network of barium borosilicate glasses brought about by the introduction of thorium and uranium ions.
© 2006 Elsevier B.V. All rights reserved.

1. Introduction

Borosilicate glasses have potential application in nuclear industry as suitable matrix for the immobilization of high-level nuclear wastes [1,2]. India has vast thorium resources amounting to about 1/3rd of the world reserve for its energy security on a sus-tainable basis. Accordingly, India has an ambitious program to use thorium in the blanket zone of fast breeder reactors at an appropriate growth of installed nuclear power in the second stage of nuclear energy program, which will be followed by introduction of Advanced Heavy Water Reactors (AHWR) based on Th–$^{233}U^{mox}$ (mixed oxide) fuel in the third stage [3]. Thorium and uranium will be among the main components present in the waste along with fission products like ^{137}Cs, ^{90}Sr, ^{106}Ru etc., which will be left over after the reprocessing of the spent fuel from reactors based on

---

* Corresponding author. Tel.: +91 22 2559 5330; fax: +91 22 2550 5151.
  E-mail address: aktyagi@barc.ernet.in (A.K. Tyagi).

Th–^{233}U^{mox} fuels [4]. This needs to be immobilized in a suitable inert matrix before their long term disposal in repositories. Borosilicate glass is one of the suitable candidates for immobilization of high level nuclear wastes, containing thorium, uranium and other fission products. No studies have been reported on the structural aspects of borosilicate glasses containing both thorium and uranium oxides, even though there are some reports on the structural aspects of borosilicate/silicate glasses incorporated with either thorium oxide or uranium oxide [5–12]. Extended X-ray absorption fine structure (EXAFS) studies on thorium incorporated silicate glasses revealed that the coordination around Th^{4+} depends on the concentration of ThO$_2$ in the borosilicate glass [5]. Recently we have reported that barium borosilicate glasses have got improved extent of ThO$_2$ incorporation compared to borosilicate glasses without BaO [6]. Based on ^{29}Si and ^{11}B MAS NMR studies, it has been inferred that Th^{4+} occupy sites which are created by non-bridging oxygen atoms (network modifying positions) in the glass, leaving the borosilicate network unaffected. This is further supported by the relatively large concentration of non-bridging oxygen atoms present in barium borosilicate glasses as revealed by the ^{17}O NMR study reported by Zhao et al. [13]. Uranium in borosilicate/aluminosilicate glasses is known to exists as U(IV), U(V) and U(VI) species, and depending up on the oxidizing or reducing environment used for glass melting, either U(VI) or U(IV) predominates in the glass matrix [7,8]. Further, the presence of ions like Ce^{4+}, Cr^{3+}, Ti^{3+} etc. also changes the relative concentration of different U species [8–10]. UV–visible-infrared absorption technique has been extensively used to identify and estimate the relative concentration of different uranium species present in the glass samples. Glancing angle EXAFS studies on borosilicate glasses containing Fe^{3+} and U^{6+} revealed that U^{6+} occupies the sites created by non-bridging oxygen atoms (network modifying positions) in the glass along with Na$^+$ ions, leaving the borosilicate network unaffected [11]. Similar behaviour of uranium ions has also been reported in ferric phosphate glasses by Mesko et al. [14].

Depending upon the oxidation state of the uranium ions, it can have different coordination polyhedra around them and this is expected to have significant effect on the structure of the glass network as well as on the extent of ThO$_2$ incorporation in the glass. Hence it will be of interest to study the structural aspects of borosilicate glasses when both uranium and thorium oxides are incorporated in it. Solid state nuclear magnetic resonance using ^{29}Si and ^{11}B as the probe nuclei combined with X-ray diffraction technique can be very effectively used for understanding the structural aspects as well as extent of ThO$_2$ incorporation in these glasses. Such studies will be helpful for the development of new glass formulations for the immobilization of wastes from the proposed nuclear reactors based on Th–U^{mox} fuels. The present work is an attempt to understand the influence of simultaneous incorporation of thorium and uranium oxide, on the structural network of barium borosilicate glass. Keeping this in mind, we have prepared barium borosilicate glasses containing a fixed concentration of ThO$_2$ (15.86 wt%) and incorporated with different amounts of uranium oxide (UO$_3$) and studied their structural aspects using ^{29}Si and ^{11}B MAS NMR and XRD techniques. ThO$_2$ amount was kept at 15.86 wt% as it is close to the optimum ThO$_2$ concentration that can be incorporated into the barium borosilicate glass without any phase separation.

2. Experimental

Required amounts of analytical grade Ba(NO$_3$)$_2$, NaNO$_3$, SiO$_2$ and H$_3$BO$_3$ were taken so as to get the base glass with a composition (SiO$_2$)$_{0.39}$(B$_2$O$_3$)$_{0.25}$(Na$_2$O)$_{0.12}$(BaO)$_{0.24}$ and mixed with required amounts of Th(NO$_3$)$_4$ · 5H$_2$O and UO$_3$, ground well and heated at 1000 °C for 4 h in siliminite crucibles. The free flowing melt was quenched between two stainless steel plates. For all the glass samples, the ratio of Na$_2$O to BaO and SiO$_2$ to B$_2$O$_3$ were maintained constant, and are 0.5 and 1.56, respectively. Further the constituents of the glass formulations were proportionately changed in such a way that SiO$_2$/Na$_2$O, SiO$_2$/B$_2$O$_3$, SiO$_2$/BaO, B$_2$O$_3$/Na$_2$O and B$_2$O$_3$/BaO are same for all the samples with different amounts of ThO$_2$ and UO$_3$. X-ray diffraction patterns were recorded using a Philips PW1710 X-ray diffractometer with nickel filtered Cu-K$_\alpha$ radiation. ^{29}Si and ^{11}B MAS NMR patterns were recorded using a Bruker Avance DPX 300 machine with basic frequencies of 59.62 and 96.29 MHz, respectively. Typical 90° pulse durations employed for ^{29}Si and ^{11}B NMR experiments were 4 and 2 μs, respectively, with corresponding delay times 8 and 3 s. Powdered samples were packed inside zirconia rotors and subjected to a spinning speed of 5 kHz for MAS NMR experiments. ^{11}B static

NMR patterns were also recorded with same pulse duration and delay times as that used for MAS NMR experiments. ^{11}B NMR experiments were also carried out with lower pulse durations (up to 0.3 μs) and the line shapes were found to be identical. Static ^{11}B NMR patterns were simulated using the WINFIT program supplied by Bruker. The chemical shift values for ^{29}Si and ^{11}B NMR patterns are reported with respect to tetramethylsilane and 1 M aqueous solution of H_3BO_3, respectively. All the ^{11}B NMR patterns were corrected for the boron nitride (BN) background arising from the Bruker MAS NMR probe.

3. Results and discussion

Fig. 1 shows the representative XRD patterns for barium borosilicate glasses containing different amounts of thorium and uranium oxides. Barium borosilicate glass without any thorium and uranium oxides showed a broad peak around 2θ value of 13° characteristic of amorphous borosilicate network.
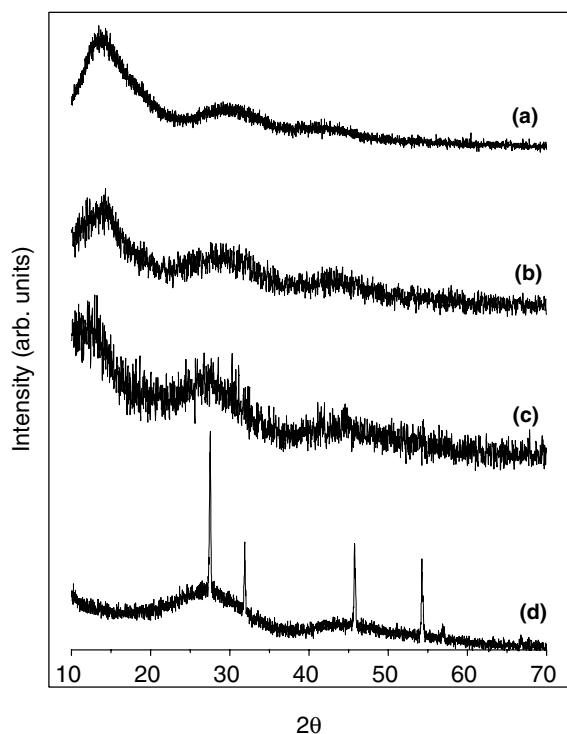

Fig. 1. XRD patterns for barium borosilicate glasses containing (a) no thorium and uranium oxides, (b) 15.86 wt% ThO_2 and 5 wt% uranium oxide, (c) 15.86 wt% ThO_2 and 7.5 wt% uranium oxide and (d) 15.86 wt% ThO_2 and 10.0 wt% uranium oxide.

With incorporation of thorium and uranium oxides, diffraction patterns became too noisy and broad indicating the distortion of the borosilicate network brought about by the uranium and thorium ions. Above 7.5 wt% uranium oxide incorporation, phase separation in the glass took place as revealed by the sharp peaks observed around 2θ values 27.53°, 31.89°, 45.77° and 54.25° etc. The sharp peaks have been attributed to the presence of crystalline ThO_2 phase [15] in the glassy matrix.

Fig. 2 shows the ^{29}Si MAS NMR patterns for barium borosilicate glasses containing 15.86 wt% of thorium oxide and incorporated with varying amounts of uranium oxide. For the purpose of comparison, the glass sample without any thorium and uranium oxide incorporation is also shown. Barium borosilicate glasses without any thorium and uranium oxide showed a broad asymmetric peak around −92 ppm. Deconvolution based on a Gaussian fit resulted in two peaks around −98 and −89 ppm characteristic of the Q^3 and Q^2 structural units of silicon, respectively, (where Q^n represents silicon structural units having 'n' bridging oxygen atoms) [6,16,17]. The relative concentration of both the structural units is indicated below the corresponding peaks. With 15.86 wt% incorporation of ThO_2 in the glass, the relative concentration of Q^3 and Q^2 structural units remained unaffected (within experimental errors) as can be seen from Fig. 2(b), suggesting that thoria incorporation does not result in the breakage of Si–O–Si linkages. Th^{4+} ions must be occupying some of the sites created by non-bridging oxygen atoms (network modifying positions) in the glass, without affecting the borosilicate network. With incorporation of 5 wt% of uranium oxide in the thorium oxide incorporated glass, the ^{29}Si MAS NMR line shape changes and based on the deconvolution of the NMR pattern it can be seen that, the relative concentration of Q^2 structural units increases at the expense of Q^3 structural units. With further increase in uranium oxide concentration, the relative concentration of both Q^2 and Q^3 structural units and their chemical shift values remained unaffected as can be seen from the identical line shapes in Fig. 2(c)–(e). Identical chemical shift values for both Q^2 and Q^3 structural units of silicon with increase in uranium oxide concentration suggest that there is no direct interaction between silicon and uranium structural units and uranium ions probably occupy the sites created by the significant number of non-bridging oxygen atoms present in the glass (network modifying sites). There is no
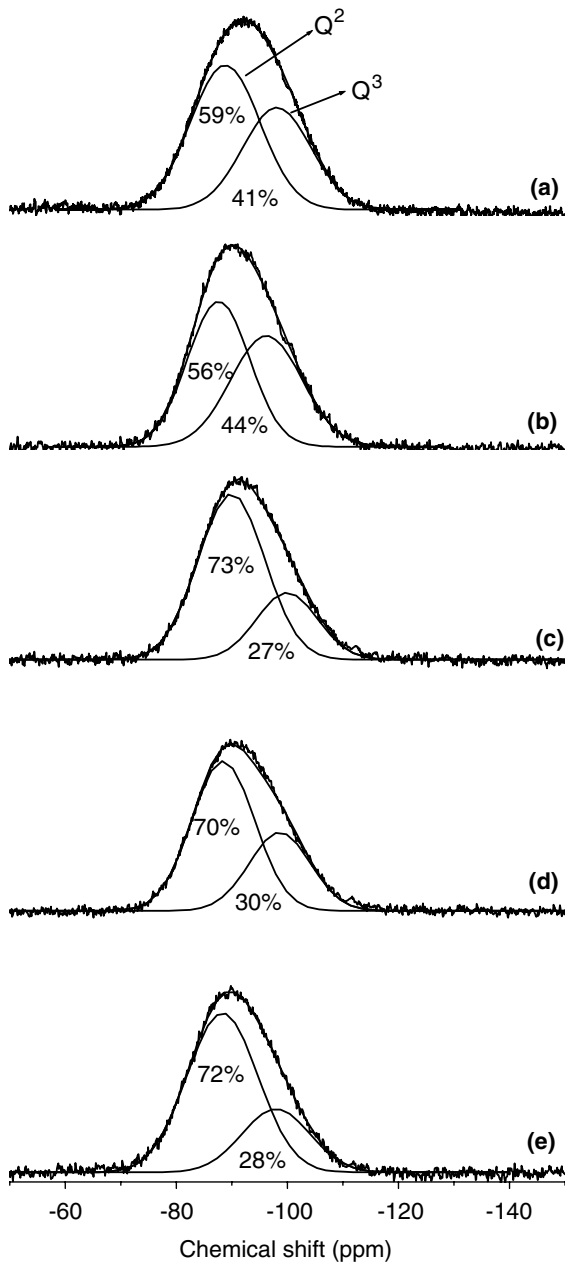
Fig. 2. ^{29}Si MAS NMR Patterns for barium borosilicate glasses containing (a) no thorium and uranium oxides, (b) 15.86 wt% ThO$_2$, (c) 15.86 wt% ThO$_2$ and 5 wt% uranium oxide (d) 15.86 wt% ThO$_2$ and 7.5 wt% uranium oxide and (e) 15.86 wt% ThO$_2$ and 10.0 wt% uranium oxide. Relative concentration of Q^3 and Q^2 structural units are indicated below each peak.
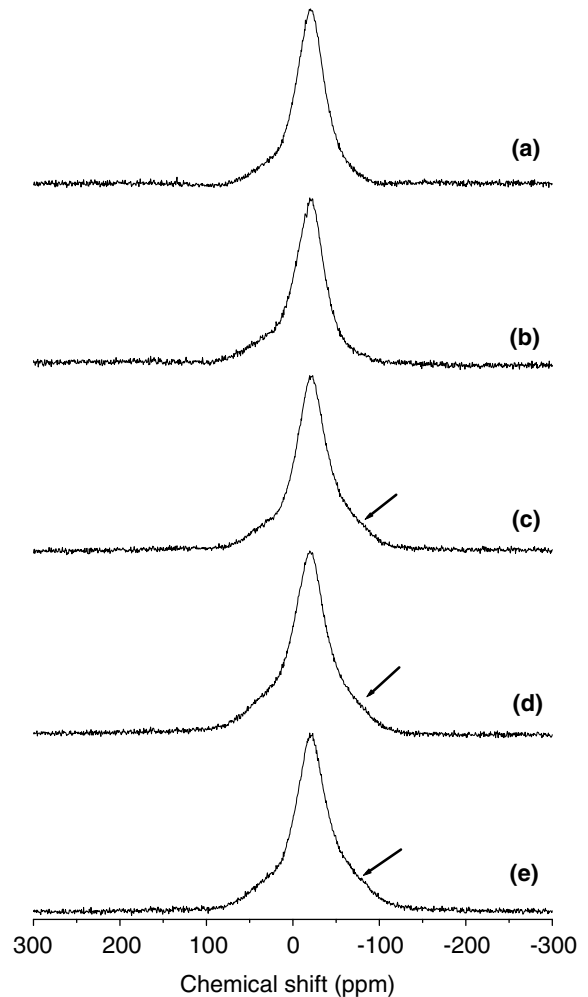

Fig. 3. ^{11}B static NMR patterns for barium borosilicate glasses containing (a) no thorium and uranium oxides, (b) 15.86 wt% ThO$_2$, (c) 15.86 wt% ThO$_2$ and 5 wt% uranium oxide, (d) 15.86 wt% ThO$_2$ and 7.5 wt% uranium oxide and (e) 15.86 wt% ThO$_2$ and 10.0 wt% uranium oxide. The arrows represent the region where the line shape change is taking place.

change in the ^{29}Si MAS NMR line shape even after partial phase separation of ThO$_2$ from the glass matrix.

Fig. 3 shows the static ^{11}B static NMR patterns for barium borosilicate glasses incorporated with 15.86 wt% ThO$_2$ and containing different amounts of uranium oxide along with that of the glass sample without any thorium and uranium oxides. The patterns essentially consist of a relatively sharp peak superimposed over a broad peak appearing as shoulders on both sides of the sharp peak. As ^{11}B is a quadrupolar nuclei ($I = 3/2$) tetrahedrally coordinated boron structural units (BO$_4$) by virtue of their cubic symmetry have got negligible quadrupolar interaction thereby resulting in sharp peak in the NMR spectrum corresponding to such structural units. Unlike this for BO$_3$ structural units, due to the non-cubic symmetry, significant quadrupolar

interaction results in the broadening of the NMR line shapes. For the glass samples which do not have any thorium or uranium oxides and those incorporated with 15.86 wt% thorium oxide, ^{11}B static patterns are almost same, indicating that relative concentration of BO_3 and BO_4 structural units are unaffected by incorporation of ThO_2 alone in the glass. However with the addition of uranium oxide, the relative intensity of the shoulder slightly increases (the arrows shown in the patterns denote the region where the changes are taking place) as revealed by the careful observation of the patterns
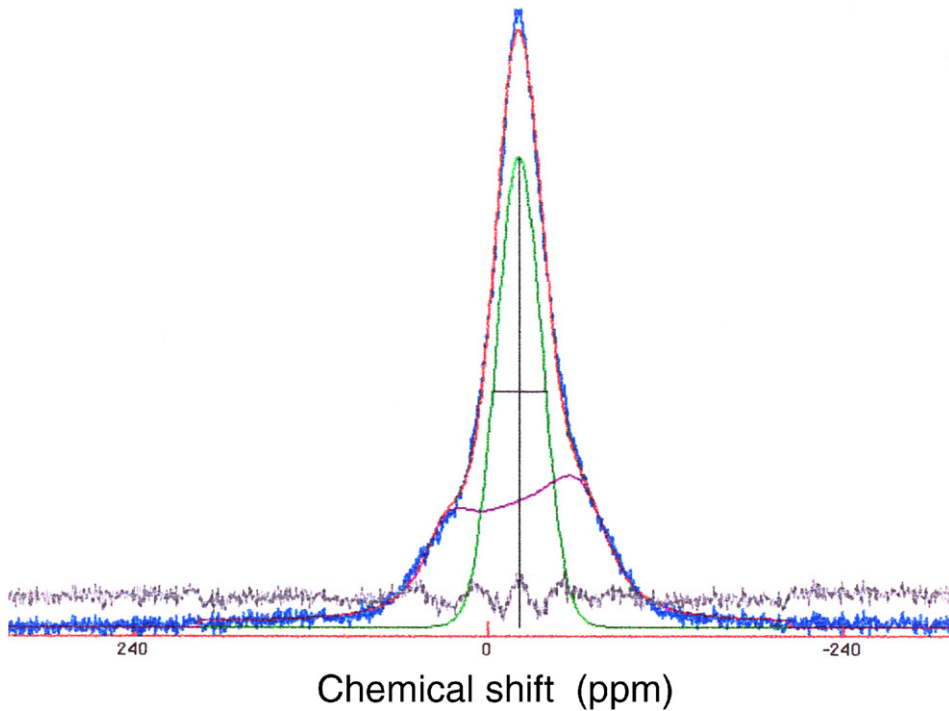

Fig. 4. Simulated ^{11}B static NMR pattern for a representative barium borosilicate glass containing 15.86 wt% ThO_2 and 5 wt% uranium oxide. Blue line: experimentally obtained NMR pattern, Violet line: characteristic of BO_3 structural units, Green line: characteristic of BO_4 structural units, Red line: Overall simulated pattern and the black line is the residuals (difference between the experimental and simulated patterns). (For interpretation of the references in colour in this figure legend, the reader is referred to the web version of this article.)

Table 1
Relative concentration of BO_3 and BO_4 structural units along with their chemical shift values

Nominal compositions (in wt%) of ThO_2 and UO_3	δ_{BO_4} (ppm) (± 1)[a]	Line width (ppm)	% of BO_4	δ_{BO_3} (ppm) (± 1)[a]	C_q (MHz) (± 0.1)[a]	% of BO_3	Asymmetry parameter (η) (± 0.1)[a]
ThO_2: 0 UO_3: 0	−20.8	34.5	57.3	3.3	2.37	42.7	0.6
ThO_2: 15.86 UO_3: 0	−20.8	34.5	53.2	2.0	2.43	46.8	0.7
ThO_2: 15.86 UO_3: 5.0	−20.9	36.1	47.1	−3.5	2.72	52.9	0.2
ThO_2: 15.86 UO_3: 7.5	−18.7	36.6	39.7	−4.1	2.72	60.3	0.3
ThO_2: 15.86 UO_3: 10.0	−20.5	36.0	41.4	−3.0	2.75	58.6	0.2

Quadrupole coupling constant (C_q) and asymmetry parameter (η) for BO_3 structural units are also shown. Errors in the relative concentration of BO_3 and BO_4 structural units are around 2–3%.

[a] Errors have been obtained by carrying out duplicate NMR measurements.

shown in Fig. 3(c)–(e). ^{11}B static NMR patterns have been simulated assuming a Gaussian–Lorentzian line shape with negligible quadrupole coupling constant for BO_4 structural units and a single quadrupolar broadened line shape for the trigonally coordinated boron structural units. As the line shapes for symmetric BO_{3S} (trigonal boron structural units attached with three bridging oxygen atoms) and asymmetric BO_{3A} (trigonal boron structural units attached with both bridging and non-bridging oxygen atoms) are almost same no distinction was made between symmetric BO_{3S} and asymmetric BO_{3A}. A similar procedure was also employed by Miyoshi et al. [18] for simulating the ^{11}B NMR patterns from sodium borosilicate glasses containing CaO. Experimental and simulated ^{11}B NMR patterns for a representative sample having 5 wt% uranium oxide incorporation is shown in Fig. 4. The fitting parameters namely the chemical shift values and the relative concentration of BO_3 and BO_4 structural units along with the quadrupole coupling constant (C_q) and asymmetry parameter (η) for BO_3 structural units present in all the samples are shown in Table 1. The chemical shift values and line widths for BO_4 structural units remained almost same within experimental errors for all the glass samples as can be seen from Table 1. However the intensity of the BO_4 structural units decreased systematically with increase in uranium oxide incorporation up to 7.5 wt% and above this concentration, the relative concentration of BO_4 structural units remained almost same. The decrease in BO_4 structural units is associated with increase in relative concentration of BO_3 structural units (see Table 1). The quadrupole coupling constant C_q for BO_3 structural units remained more or less same for both barium borosilicate and thorium oxide incorporated barium borosilicate glasses. However with uranium oxide incorporation, the C_q values increase significantly as can be seen from Table 1. The observed increase in the C_q values suggests that the BO_3 structural units in the borosilicate network undergo significant distortion with uranium oxide incorporation in the glass. The chemical shift values of BO_3 structural units δ_{BO_3} decreases with increase in UO_3 concentration in the glass and this has been attributed to the increase in B–O–B chain length brought about by the increase in relative concentration of BO_3 structural units. Similar decrease in ^{31}P chemical shift values were also reported for phosphate based glasses with increase in P–O–P chain length [19]. Asymmetry parameter (η) for BO_3

structural units is also found to change with uranium oxide incorporation in the glass. However at
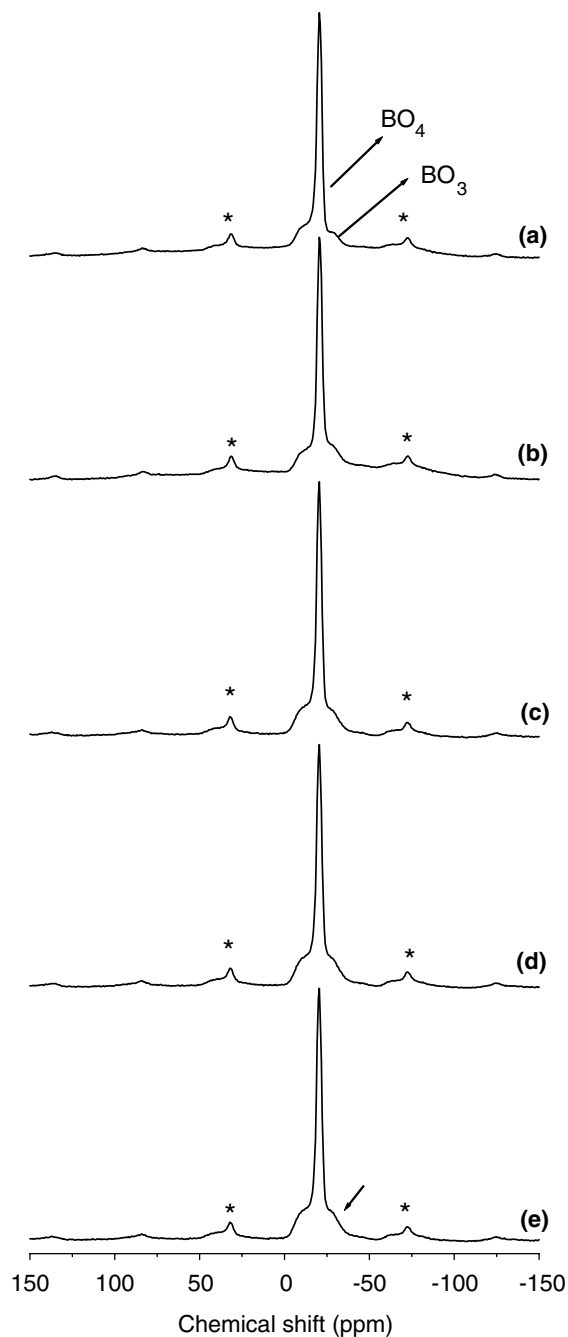

Fig. 5. ^{11}B MAS NMR Patterns for barium borosilicate glasses containing (a) no thorium and uranium oxides, (b) 15.86 wt% ThO_2, (c) 15.86 wt% ThO_2 and 5 wt% uranium oxide, (d) 15.86 wt% ThO_2 and 7.5 wt% uranium oxide and (e) 15.86 wt% ThO_2 and 10.0 wt% uranium oxide. Peaks marked '*' are spinning sidebands. The arrow represents the region where the line shape change is taking place.

this stage we do not have an explanation for the variation of the asymmetry parameter with uranium oxide content for these glasses.

Fig. 5 shows the ^{11}B MAS NMR patterns for barium borosilicate glasses containing 15.86 wt% thorium oxide and different amounts of uranium oxide. Like ^{11}B static NMR patterns, MAS NMR patterns consist of sharp peaks ~-20 ppm with less intense broad shoulders on both sides of the sharp peak along with sidebands. Based on the explanation described above for the static ^{11}B NMR patterns, the sharp peak has been attributed to the BO_4 structural units and the broad shoulders to the BO_3 structural units. Due to the poor detection efficiency of BO_3 structural units in MAS NMR experiments, the changes in line shape brought about by the relative increase in BO_3 structural units are not apparent. However, a careful look at the ^{11}B MAS NMR patterns of Fig. 5(a) and (e) reveal that there is a slight increase in the relative intensity of the peak corresponding to BO_3 structural units compared to that of BO_4 structural units (denoted by an arrow in Fig. 5(e)) when thorium and uranium oxides are incorporated into the barium borosilicate glass. The calculation of the relative concentration of BO_3 and BO_4 structural units were not attempted, as there is a significant loss of intensity for BO_3 structural units from the isotropic peak, due to the presence sidebands.

4. Conclusions

Based on ^{29}Si MAS NMR studies on ThO_2 containing barium borosilicate glasses having varying amounts of uranium oxides, it has been concluded that uranium oxide incorporation is associated with the conversion of Q^3 to Q^2 structural units of silicon and the increased number of non-bridging oxygen atoms thus produced favours the uranium ions to occupy the sites which are created by the non-bridging oxygen atoms (network modifying sites) in the glass. Simulation of the ^{11}B static NMR patterns established that with increase in uranium oxide concentration in the glass, BO_4 structural units get converted to BO_3 structural units with significant distortion. Above 7.5 wt% of uranium oxide incor-

poration in the glass, resulted in the phase separation of ThO_2 as revealed by XRD studies.

References

[1] P.G. Eller, G.O. Tarvinen, J.D. Purson, R.A. Penneman, R.R. Ryan, F.W. Lytle, R.B. Greegor, Radiochim. Acta 39 (1985) 17.
[2] A.J. Freeman, G.H. Lander (Eds.), Handbook on the Physics and Chemistry of the Actinides, Elsevier, 1987, p. 271.
[3] A. Kakodkar, in: Proceedings of international seminar on the role of Nuclear Energy for sustainable development New Delhi, India, 1997, p. 62.
[4] B. Bhattacharjee, in: Proceedings of Conference on Nuclear Fuel Cycle, INSAC-2003, (Kalpakkam, India, 2003).
[5] F. Farges, Geochim. Cosmochim. Acta 55 (1991) 3303.
[6] (a) R.K. Mishra, V. Sudarsan, A.K. Tyagi, C.P. Kaushik, K. Raj, S.K. Kulshreshtha, J. Non-Cryst. Solids 35 (2006) 2952;
(b) R.K. Mishra, P. Sengupta, C.P. Kaushik, A.K. Tyagi, G.B. Kale, K. Raj, J. Nucl. Mater, accepted for publication.
[7] H.D. Schreiber, G.B. Blazs, Phys. Chem. Glasses 23 (1982) 139.
[8] H.D. Schreiber, G.B. Blazs, P.L. Jamison, A.P. Shaffer, Phys. Chem. Glasses 23 (1982) 147.
[9] H.D. Schreiber, J. Non-Cryst. Solids 49 (1982) 189.
[10] H.D. Schreiber, G.B. Blazs, S.J. Kozak, J. Am. Ceram. Soc. 66 (1983) 340.
[11] G.N. Greaves, J. Non-Cryst. Solids 120 (1990) 108.
[12] G.S. Knapp, B.W. Veal, D.J. Lam, A.P. Paulikas, H.K. Pan, Mater. Lett. 2 (1984) 253.
[13] P. Zhao, S. Kroeker, J.F. Stebbins, J. Non-Cryst. Solids 276 (2000) 122.
[14] M.G. Mesko, D.E. Day, J. Nucl. Mater. 273 (1999) 27.
[15] Joint Committee for Powder Diffraction Standards, Card No: 42-1462.
[16] V.K. Shrikhande, V. Sudarsan, G.P. Kothiyal, S.K. Kulshreshtha, J. Non-Cryst. Solids 283 (2001) 18.
[17] V. Sudarsan, V.K. Shrikhande, G.P. Kothiyal, S.K. Kulshreshtha, J. Phys.: Condens. Matter. 14 (2002) 6553.
[18] H. Miyoshi, D. Chen, H. Masui, T. Yazawa, T. Akai, J. Non-Cryst. Solids 345&346 (2004) 99.
[19] V. Sudarsan, R. Mishra, S.K. Kulshreshtha, J. Non-Cryst. Solids 342 (2004) 160.